Military Technical College
Kobry El-Kobbah,
Cairo, Egypt.

13th International Conference on Applied Mechanics and Mechanical Engineering.

DAMAGE PREDICTION OF AXIALLY CRUSHED CORRUGATED FRUSTA

YOUNES* M.M.A.

ABSTRACT

Failure analysis of corrugated shells requires knowledge of the behavior of a shell structure as it is crushed. Investigation of this problem is presented in this paper. The axial crushing of a right circular axi-symmetric corrugated frusta subjected to quasi-static compression is numerically studied. The finite element code ABAQUS/Explicit was employed to predict the crushing behavior and the effect of different geometric parameters required to enhance the energy absorption capability of corrugated frusta. The main objectives are to establish the load-deflection response of the axi-symmetric corrugated frusta and to describe the overall deformation of the frusta, since this data greatly affect the energy absorbed by frustum models. The present simulation also provides a simple demonstration of the capabilities of ABAQUS/Explicit for modeling contact problems between deformable bodies and rigid, impenetrable surfaces. Results showed that as the number of corrugations along a frustum generator increases, the amount of absorbed energy significantly increases, however the collapse modes of those corrugated frusta are qualitatively similar. The influence of varying the axial length-to-thickness ratio and the corrugation angle on the crashworthiness performance of frustum models are predicted and the obtained finite element results are depicted and assessed.

KEY WORDS

Finite element; Corrugated frusta; Axial loading; Energy absorption; Collapse

---

* Egyptian Armed Forces.

INTRODUCTION

Frusta (truncated circular cones) have wide ranges of applications among the most efficient energy absorption structural members [1]. Mamalis et al. [2-4] reported experimental results of axial crushing of aluminum and steel cylinders and frusta and an expression has been introduced for the crushing load by fitting the experimental results corresponding to axi-symmetric and diamond failure modes. Mamalis et al. [5-6] used kinematics to study the collapse mechanism in PVC tubes and frusta subjected to axial load. El-Sobky and Singace [7] examined experimentally the stress distribution of elastically loaded frusta subjected to axial loading. The energy absorption characteristics and the collapse modes of axially crushed frusta of different geometric ratios and end-constraints were depicted quasi-statically [8] and dynamically [9].

Much research effort was done on introducing corrugation along the shell generator to enhance the crashworthiness performance of shell structures [1]. Crashworthiness is defined as the ability of a restraint structure to withstand loads below a certain level and to reduce the damage produced from exposing this structure to excessive loads [10]. The behavior of corrugated structures subjected to axial compression is greatly complicated and may involve a number of different failure mechanisms. Singace and E1-Sobky [11] improved the uniformity of the load-displacement behavior of axially crushed tubes, predict and control the mode of collapse in each corrugation in order to optimize the energy absorption capacity of the tube. Mahdi et at. [12] examined numerically the effects of parametric modifications on composite corrugated tubes and results showed that the tube's energy absorption capacity was affected significantly by varying the number of corrugation and aspect ratios. A theoretical method was built up by Liang et al. in [13] and modified in [14] to evaluate the relationship between the central deflection of a corrugated panel and external uniformly distributed pressure load including the interaction between the bending moment and the membrane force in the panel. Ross et al. [15] carried out theoretical and experimental investigations on a thin-walled corrugated carbon fibre circular cylinder in air and also under external water pressure, good agreement was found between experiment and theory.

Based on the author's knowledge, there are considerable studies have been done on energy absorption capability of corrugated plates/tubes subjected to axial loading. However, there is a lack of test results or predictions for the performance and the necessary collapse parameters of corrugated frusta models. Consequently, there is still a need for information to answer the questions arise about the actual structural behavior of axially crushed corrugated frusta. Numerical methods are now extensively applied in engineering due to the advances in computing. Of all the numerical methods, the finite element method is the most popular convenient approach, because it is easy to implement for all kinds of boundary and loading conditions and it can be used for the analysis of large complex structures.

This paper explores the crushing behavior of corrugated frusta by using the commercially available finite element code ABAQUS/Explicit version 6.4 [16]. It is interesting to note that corrugations are shaped into a series of regular folds that look like waves as shown in Fig.(1). The geometry of the corrugated frustum can easily be changed by increasing or decreasing the corrugation angle α. The main objectives are to predict the collapse mechanism of the axially crushed corrugated frusta and to examine the main different parameters affecting the energy absorption capability.

Mainly, these parameters are the number of corrugations, the corrugation angle and the frustum's axial length-to-thickness ratio.

FINITE ELEMENT MODEL

ABAQUS version 6.4 was used to predict the behavior of the axially crushed corrugated frusta. Throughout the simulation process, three different geometries of frusta have been modeled, which are straight frustum, corrugated frusta with different corrugation angles ($\alpha=5^{\circ}$: $\alpha=45^{\circ}$) and a frustum with higher number of corrugation surfaces. Moreover, different axial length-to-thickness ratio (L/t=53 : L/t=243) were used in modeling corrugated frusta. In order to verify the finite element model, the global dimensions of the corrugated frusta used in ABAQUS were essentially identical to that of the straight frustum specimens tested by El-Sobky et al. [8]. All the frusta used in the finite element simulation were constraints free with 51.6 mm top mean diameter, 151.6 mm base mean diameter and 133.7 mm axial length as shown in Figs.(1,2). The element selection process was mainly determined by the elements outputs capability to deliver the variables required in this study. The shell element S4R was used in the modelling. The element S4R is a three-dimensional, doubly curved, four-node shell element. Each node has three displacement and three rotation degrees of freedom. This element is considered a general purpose shell element because it is valid for use with both thin and thick shell problems and it allows for large strains as load increases. It is worth mentioning that all frusta models are axisymmetric. For monitoring the collapse mechanisms of frusta models, the geometry of straight frustum model is completely viewed, however the corrugated frustum with low number of corrugations is represented in a half-model view and the frustum with great number of corrugations is represented in a two-dimensional axi-symmetric model view as shown in Fig.(2). The material used in the simulation is provided from the actual material properties of frusta experimentally determined by El-Sobky et al. [8] and shown in Fig.(3). Numerical data of the mechanical properties of the material was assigned into the ABAQUS input file. Von-Mises yield criterion was applied and a list of values of the basic material properties required for this model is given in Table (1).

The other important parameter of representing crushing event is the boundary condition. In this model, free frusta have been used where the top and base sections have not been constrained. It is noted that the frusta are not completely free due to the effect of friction between the frustum model and the crushing upper and lower rigid plates. The lower rigid plate was fixed in all degrees of freedom, however the upper rigid plate was fixed in all degrees of freedom except the vertical downward displacement where the loading was applied. The applied force was then attained as a reaction and the force-displacement curve for the whole model was constructed. The progressive deformation shape was continuously monitored.

CRUSHING PROCESS

The numerical simulation is carried out by using ABAQUS/Explicit to solve a corrugated frustum model subjected to axial crushing load. ABAQUS/Explicit is a special purpose analysis product efficient for nonlinear quasi-static problems involving changes in contact conditions, such as crushing simulation. The finite element results can be assessed after completing the calculations of the reaction forces, displacements,

energy and other fundamental variables. Evaluating the simulation is generally done interactively using the visualization module of ABAQUS/CAE because it has a variety of options for displaying the results including colour contour plots, animations, deformed shaped plots and *X-Y* graphs.

VALIDATION OF THE FINITE ELEMENT MODEL

In order to insure the finite element model was sufficiently accurate, it was validated using the experimental results in Ref.[8] which depicted the gradual propagation of the collapse mechanism for an axially crushed straight frustum under quasi-static compressive loading. A typical finite element model was developed for the aluminum straight frustum specimen described in Ref.[8]. The boundary conditions of the frustum model were top constrained to nullify the radial displacement at the top, however the base of the model has not been constrained to represent identical boundary conditions to the test specimen. Figure (4) depicts the finite element frustum model with the typical dimensions of the test specimens reported in Ref.[8]. The collapse progress and the overall performance of the finite element model is almost identical to the collapse mechanism of the frustum specimen crushed quasi-statically by El-Sobky at al.[8]. Furthermore, the deformation of the two compared frusta was nearly symmetric at various compression levels as shown in Fig.(5). The validation is of particular importance, since it proves that the simulation model can be effectively used to examine the failure mechanism of a crushed frustum. The frustum response obtained by the finite element model was compared with the experimental results for a range of crash parameters as shown in Table (2). The crash parameters that have been analyzed were total compression, peak load, mean load, and total energy absorbed by the frustum. It can be seen that numerical results can predict reasonable values compared to the experimental ones. The appeared discrepancy may be attributed to the presence of imperfections in the frustum test specimens and the variation in thickness along the meridian direction of the spun frusta [17]. These imperfections were produced from the spinning process used in manufacturing of the frustum specimens. Generally, the simulation model can be effectively used to simulate the axially crushed corrugated frusta.

COLLAPSE MECHANISMS

Strength Frusta

It was proven experimentally that the straight frusta is deformed in a non-axisymmetric manner, therefore the numerical simulation was carried out with the help of three-dimensional finite element model as shown in Fig.(2.a). The load-displacement characteristics of the crushed straight frustum model accompanied by the corresponding energy absorption capacity is depicted in Fig.(6). It is noted that the collapse is initiated with the formation of an inward inverted axi-symmetric ring at the top of the frustum end as seen in Fig.(7). This inversion is accompanied by an initial peak load observed in the load-displacement curve. Progressive compression enforces the edge of the base to move radially outwards (away from the axis of frustum) and an axi-symmetric plastic hinge is formed at the contact with the lower rigid surface. It is worth mentioning that, this plastic hinge is stationary and does not roll or vary with the progress of compression. However, further compression produces a mixture of multi-

lobe and inward inversion failure modes located at the top of the model as shown in Fig.(7).

Corrugated Frusta

Apart from the straight frusta, Figs.(9,11) reveal that failure mechanisms of corrugated frusta show different characteristics. Two finite element frusta of different corrugation numbers (5 and 25) are modeled to investigate the failure mechanisms. The frustum model of 5 corrugations is represented by a half finite element model. However the results obtained from the 25 corrugations frustum model is hardly observed when using a half model. Therefore, profile of the meridian is only considered in order to display the frustum behavior during crushing as shown in Figs.(2.b,2.c).

In the initial stage of compression, the frustum model behaves as if its ends are fixed because of the influence of friction between the model edges and the rigid surfaces. Furthermore, the base of the model starts to be flattening on the lower rigid surface. Increasing the compression generates a plastic bending hinge in only one corrugation at the top of the model. Formation of the plastic hinge produces a single axi-symmetric fold at the highest corrugation which is moving with the displacement of the upper plate. During the folding of the first corrugation, the second adjacent corrugation below the first one begins slightly to be folded in the same previous manner. Folding of the second corrugation was totally carried out after the upper pate has traveled and became in contact with the current corrugation and directly pushed it downward. It is worth mentioning that, the folded corrugations part of frustum models behaves as a rigid body displaced with the upper plate however the rest of frustum models stays as a stationary rigid body in contact with the lower plate. Progressive compression reveals that, all corrugations are folded gradually in the same manner and the frustum models are collapsed in axi-symmetric accordion modes independent of the number of corrugations.

THE LOAD- AND ENERGY- DISPLACEMENT CURVES

The load-displacement curves and the corresponding absorbed energy for a straight and corrugated frusta with different number of corrugations are shown in Figs.(6,8,10). In practice this load is very important from the design point of view because it gives an indication of the force required to initiate collapse & hence begin the energy absorption process. Figure(6) of the straight frustum model shows highly non-uniform characteristics and overshoots in the load-displacement curve. It can be observed that the serrations exist in the first part of the curve (from 0.0 to 0.06m displacement) are significantly sharp and pronounced however serrations in the remaining curve became quietly slight and low. These serrations can be attributed to the elastic stiffness and the irregular deformation mechanism of the straight model. The beak value of the load was noted 4.7kN at 0.022m compression and the total absorbed energy was 250J.

The load-displacement curves in Figs.(8,10) of corrugated frusta with 5 and 25 corrugations, respectively show highly stable and uniform characteristics where the fluctuations, peaks and valleys are repeated in a regular manner. Each peak represents the localized collapse force initiated during the folding of each corrugation. Generally, the load rises steeply with upper and lower boundaries. The slope of the upper load boundary is greater than the slope of the lower load boundary in the curve of the 25

corrugations model and vice versa in the curve of the 5 corrugations model. The variation of the energy absorption capacity at different compression levels is depicted beside the load-displacement curves to establish the relation between the failure propagation and the energy absorbed by frusta until the models reach the solid length.

EFFECT OF NUMBER OF CORRUGATIONS

To investigate the number of corrugations, the mean top and bottom diameters of frusta, the model thickness and its axial length are keeping constant with the same dimensions depicted in Fig.(1). Regular corrugations are a condition in all simulations curried out in this paper. The deformation mechanism and the energy absorption capacity of the corrugated frustum with 5 corrugations are compared with that of the 25 corrugations. It was found that, the two corrugated frusta of 5 and 25 corrugations are crushed in a similar regular manner with axi-symmetric accordion failure modes as shown in Figs.(9,11). However, the number of corrugations factor was found to have a significant role in the frustum energy absorption capacity. The finite element model with higher number of corrugations which is 25, absorbed more energy (245 J) compared to the model with 5 corrugations (30 J) as shown in Fig.(12). Hence, the deformation shape of a corrugated frustum is independent on the number of corrugations, while increasing the number of corrugations increases the capability of the frustum to absorb energy.

EFFECT OF CORRUGATION ANGLE α

Ten models with different corrugation angles α were simulated in order to examine the effect of changing the corrugation angle on the frustum energy absorption capacity. The model drawn in Fig.(1) was employed for this study. The variation of the absorbed energy of the corrugated frusta with different corrugation angles ranged from 0° to 45° is shown in Fig.(13). This figure may be divided into three zones in order to have the ability to describe various relations. In zone (1) ($\alpha = 0^{\circ}$-10°) as the corrugation angle α decreased the amount of energy absorbed by a frustum model is sharply increased. During zone (2) ($\alpha = 10^{\circ}$-35°) a steeply decreasing by 30% in the energy absorption capacity is noted with the increasing of the frustum corrugation angle. It is observed in zone (3) ($\alpha = 35^{\circ}$-45°) a localized overshoot in the amount of energy absorbed for a frustum model with 40° corrugation angle. These various relations may be attributed to the natural resistance of the corrugation geometry itself to the applied load during crushing process. Generally, the corrugation angle α plays a significant role in the energy absorption capacity of frusta.

EFFECT OF FRUSTUM LENGT-THICKNESS RATIO L/t

The other important parameter that needs to be given equal attention is the wall thickness of frustum model. Therefore, six finite element corrugated models of different length-to-thickness ratio L/t ranged from 50 to 250 were examined. This numerical simulation was carried out on the finite element model depicted in Fig.(1). It is found that decreasing the length-to-thickness ratio L/t causes a significant increase in the amount of energy absorbed by models. Figure (15) shows the accumulative energy absorbed by different L/t corrugated frusta at various deformation levels. These energy-

displacement curves are calculated by integrating the area under the obtained load-displacement curves shown in Fig.(14). It is observed that all frustum models have a similar load-displacement characteristics and the energy absorption capacity increases with increasing deformation level. Furthermore, similar behavior of the load-displacement curves in Fig.(14) reveals and confirms the similarity of the collapse mechanisms of frustum models independent of the frustum length-to-thickness ratio L/t. For higher values of L/t (134-243), the amount of energy absorbed by models is relatively small compared with the smaller values of L/t (53-67). Moreover, corrugated frusta with high L/t collapse easily since the structure becomes weak due to its low wall resistance towards the applied compression. However, decreasing the frustum length-to-thickness ratio L/t affects the crushing force because the frustum wall becomes dense and higher load is required to overcome the material densification.

CONCLUSION

The quasi-static axial loading of corrugated aluminum frusta compressed between two parallel flat rigid plates is investigated numerically by using the finite element code ABAQUS/Explicit. ABAQUS succeeded to simulate the multi-lobe and inward inversion failure mode of the straight frustum compared with the experimental one. However, the collapse mechanism of the corrugated frustum model is predicted in an axi-symmetric accordion failure mode, independent of the number of corrugations. The predicted load-displacement curve of each corrugated frustum model has a number of peaks equal to the number of corrugations of the investigated model. The amount of energy absorbed by the 25 corrugations frustum is highly greater than that absorbed by the 5 corrugations one. In other words, increasing the number of corrugations will increase the energy absorption capacity of the corrugated frusta. Crushing behavior of the corrugated frustum is significantly affected by the corrugation angle α. A sharp increasing in the energy absorption capacity of corrugated frusta is observed with the decreasing of the corrugation angle $\alpha < 10^{\circ}$, however the amount of energy absorbed is steeply decreased up to $\alpha = 35^{\circ}$. A local jump in the absorbed energy is noted at $\alpha = 40^{\circ}$ and the minimum value of energy absorbed by the corrugated frustum is presented at $\alpha = 45^{\circ}$. The axial length-to-thickness ratio L/t plays an effective role in enhancement the energy absorbed by the corrugated frusta. Decreasing the ratio of L/t increases the energy absorption capacity of the corrugated frustum models.

REFERENCES

[1] Alghamdi, A.A.A., “Collapsible Impact Energy Absorbers: an Overview”, Thin-Walled Structures, Vol. 39, pp. 189-213, 2001.

[2] Mamalis A. G. and Johnson W., “The Quasi-static crumpling of thin walled circular cylinders and frusta under axial compression”, Int. J. Mech. Sci., Vol. 25, No. 9, pp. 713-732, 1983.

[3] Mamalis A.G., Johnson W. and Viegelahn G. L., “The crumpling of steel thin-walled tubes and frusta under axial compression at elevated strain-rate: some experimental results”, Int. J. Mech. Sci., Vol. 26, No. 11/12, pp. 537-547, 1984.

[4] Mamalis A. G., Manolakos D.E., Saigal S., Viegelahn G. and Johnson W., “Extensible plastic collapse of thin-wall frusta as energy absorbers”, Int. J. Mech. Sci., Vol. 26, No. 4, pp. 219-229, 1986.

[5] Mamalis A. G., Manolakos D. E., Viegelahn G.L., Vaxevanidis N.M. and Johnson W., "On the axial collapse of thin-walled PVC conical shells", Int. J. Mech. Sci., Vol. 28, No. 6, pp. 323-335, 1986.
[6] Mamalis A. G., Manolakos D. E., Viegelahn G. L. and Johnson W., "The modelling of the progressive extensible plastic collapse of thin-wall shells", Int. J. Mech. Sci., Vol. 30, No. 3/4, pp. 249-261, 1988.
[7] El-Sobky H. and Singace A. A., "An Experiment on Elastically Compressed Frusta", Thin-Walled Structures, Vol. 33, No. 4, pp. 231-244, 1999.
[8] El-Sobky H., Singace A. A. and Petsios M., "Mode of Collapse and Energy Absorption Characteristics of Constrained Frusta under Axial Impact Loading", Int. J. Mech. Sci., Vol. 43, No. 3, pp. 743-757, 2001.
[9] Singace A. A., El-Sobky H. and Petsios M., "Influence of End Constraints on the Collapse of Axially Impacted Frusta", Thin-Walled Structures, Vol. 39, pp. 415-428, 2001.
[10] Jones N., "Structural impact", Cambridge, UK: Cambridge University Press; 1989.
[11] Singace A. A. and E1-Sobky H., "Behavior of Axially Crushed Corrugated Tubes", Int. J. Mech. Sci., Vol. 39, No. 3, pp. 249-268, 1997.
[12] Mahdi E., Mokhtar A. S., Asari N. A., Elfaki F. and Abdullah E. J., "Nonlinear Finite Element Analysis of Axially Crushed Cotton Fiber Composite Corrugated Tubes", Composite Structures, Vol. 75, pp. 39-48, 2006.
[13] Liang Y. H., Louca L. A. and Hobbs R. E., "A Simplified Method in the Static Plastic Analysis of Corrugated Steel Panels", J. Strain Anal. Eng Des., Vol. 41, No. 2, pp. 135-149, 2006.
[14] Liang Y. H., Louca L. A. and Hobbs R. E., "Corrugated Panels under Dynamic Loads", Int. J. Impact Eng., Vol. 43, pp. 1185-1201, 2007.
[15] Ross C. T. F., Little A. P. F., Koster P. and Tewkesbury G., "Vibration of a Thin-Walled Carbon Fiber Corrugated Circular Cylinder under External Water Pressure", Thin-Walled Struct., Vol. 44, pp. 542-553, 2006.
[16] Hibbitt H. D., Karlsson B. I. and Sorenson Inc., "ABAQUS/Explicit User's Manual, Version 6.4", 2003.
[17] Easwara Prasad G.L. and Gupta N.K., "An Experimental Study of Deformation Modes of Domes and Large-Angled Frusta at Different Rates of Compression", Int. J. Impact Eng., Vol. 32, pp. 400-415, 2005.

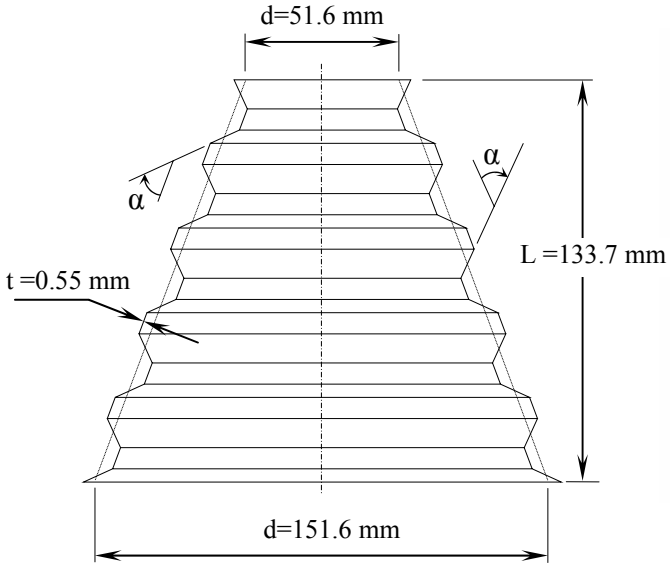

Fig.(1) Corrugated frustum

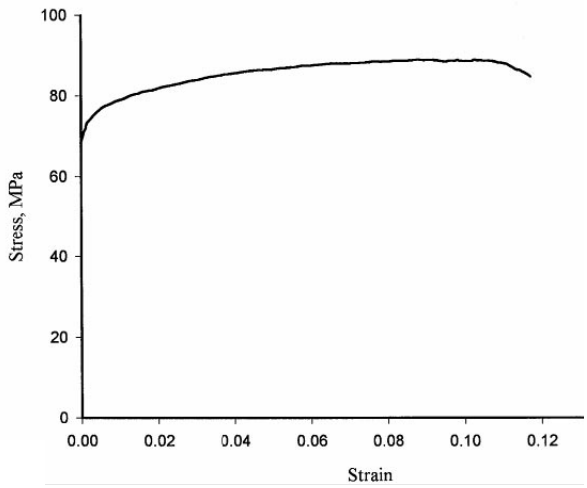

Fig.(3) A typical stress-strain curve for aluminum alloy [8]

Table.(1) Material properties required for finite element model

	Stress (σ) MPa	Strain (ε)
Young's modulus E = 69 GPa	70	0.00
	80	0.02
Density ρ = 2690 kg/m^3	82	0.04
	84	0.06
Poisson's ratio v = 0.3	86	0.08
	87	0.10
	88	0.11
	82	0.12

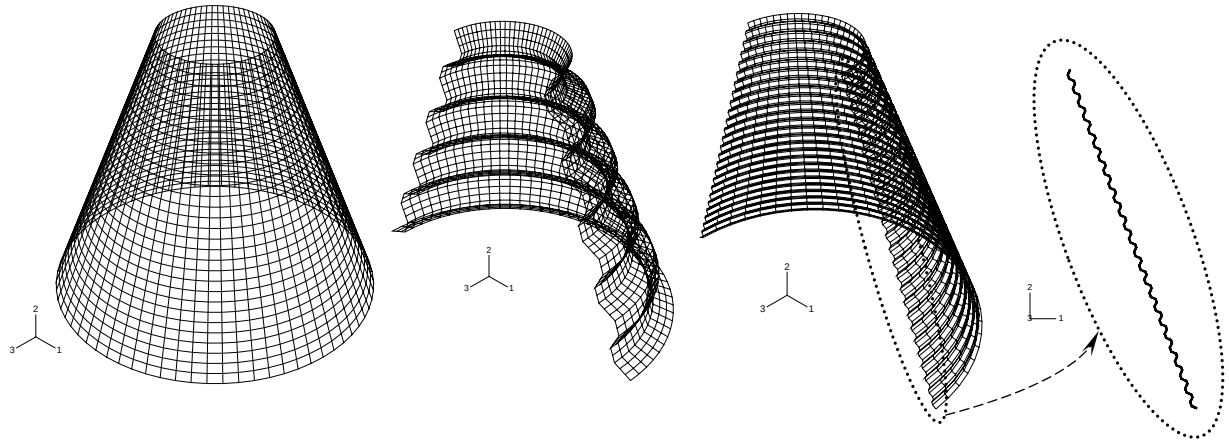

(a) Straight frustum (b) Corrugated frustum (5 corrugations) (c) Corrugated frustum (25 corrugations)

Fig.(2) Three-dimensional finite element frusta modeled by ABAQUS

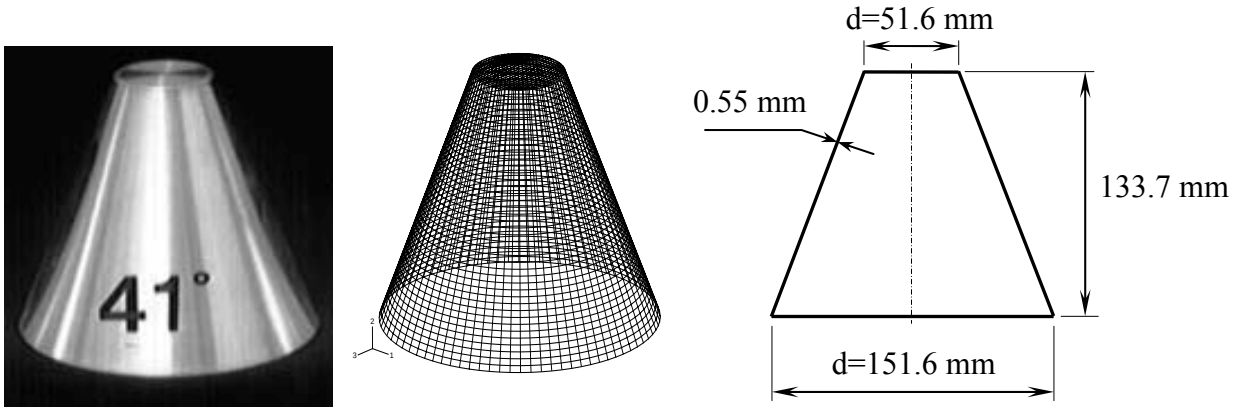

Fig.(4) Top constrained finite element straight frustum model
used to simulate the straight frustum specimen in Ref.[8]

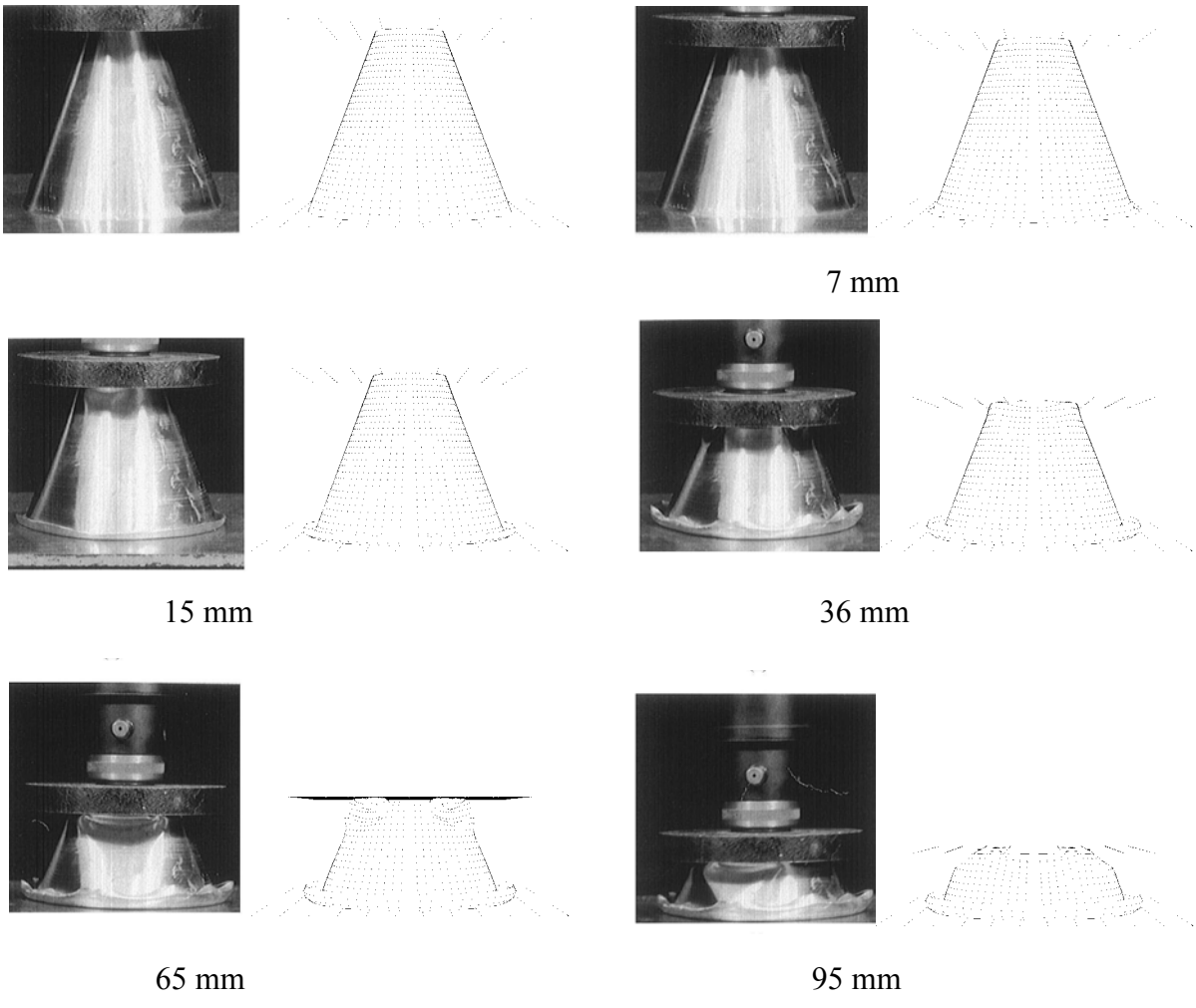

Fig.(5) Gradual crushing of the top constrained straight frustum
using the present ABAQUS solution and the experimental results in Ref.[8]

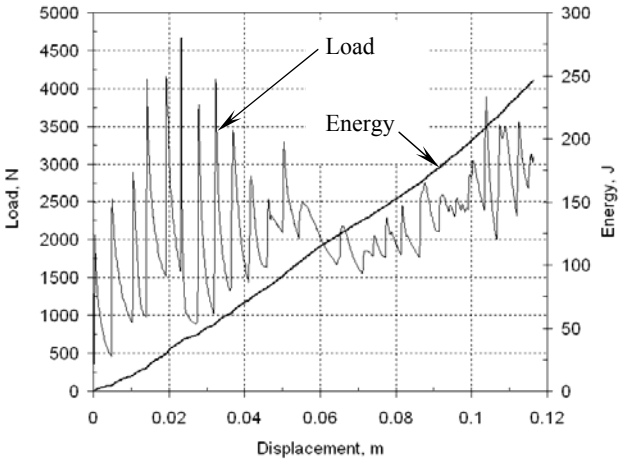

Fig.(6) Load- and energy-displacement curves of the straight frustum model

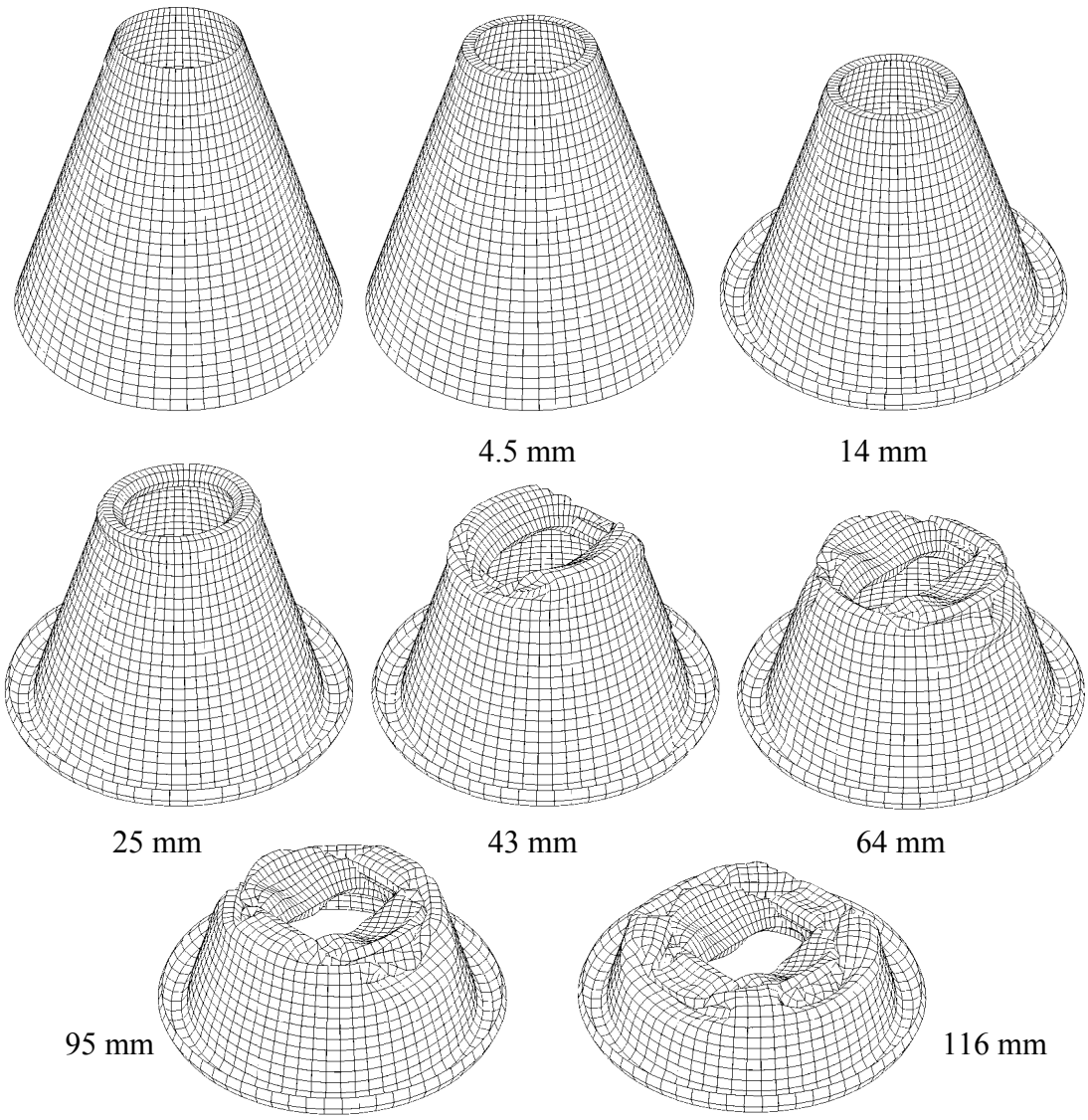

Fig.(7) Collapse mechanism of the straight frustum model

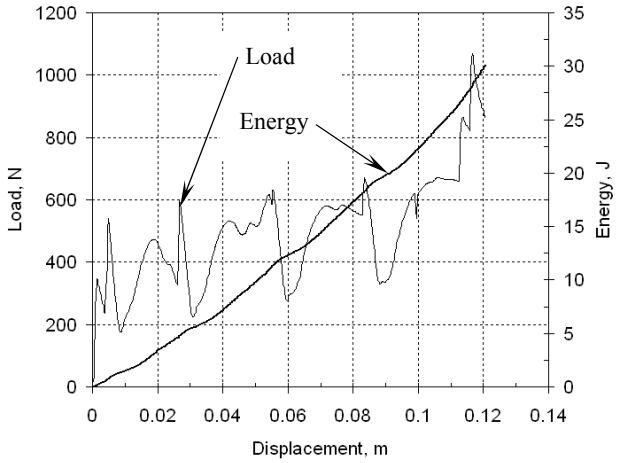

Fig.(8) Load- and energy-displacement curves of the 5 corrugations frustum model

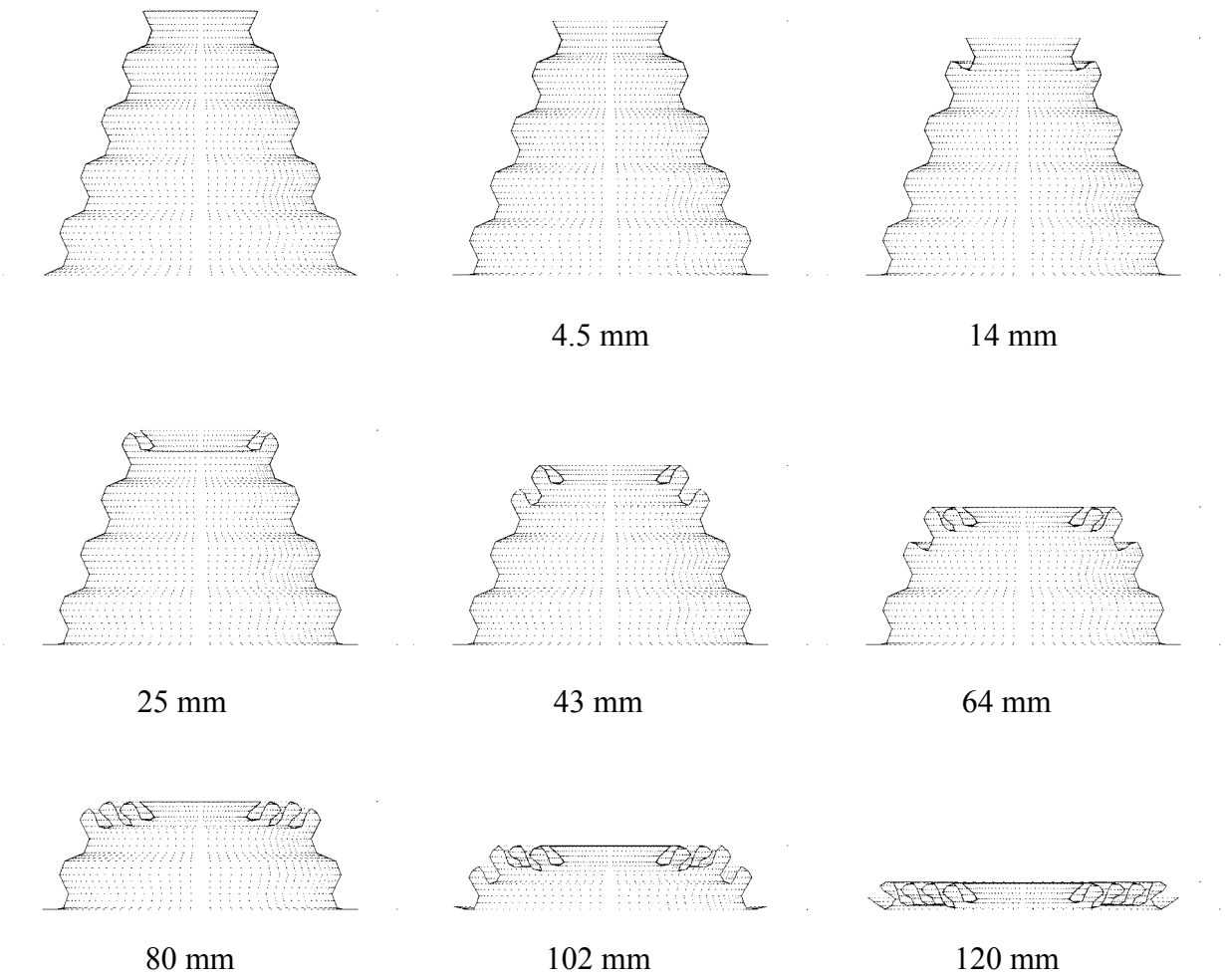

Fig.(9) Collapse mechanism of the 5 corrugations frustum model

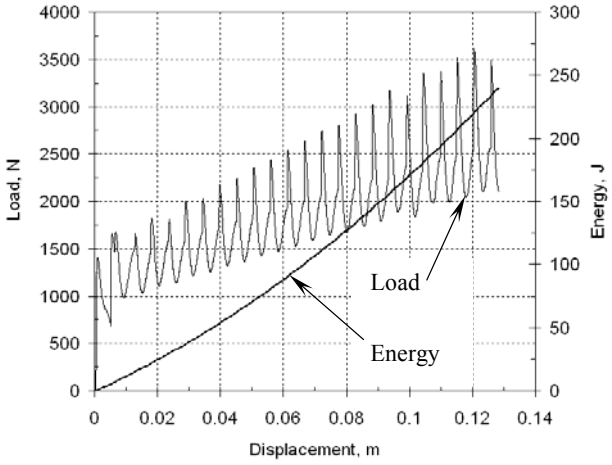

Fig.(10) Load- and energy-displacement curves of the 25 corrugations frustum model

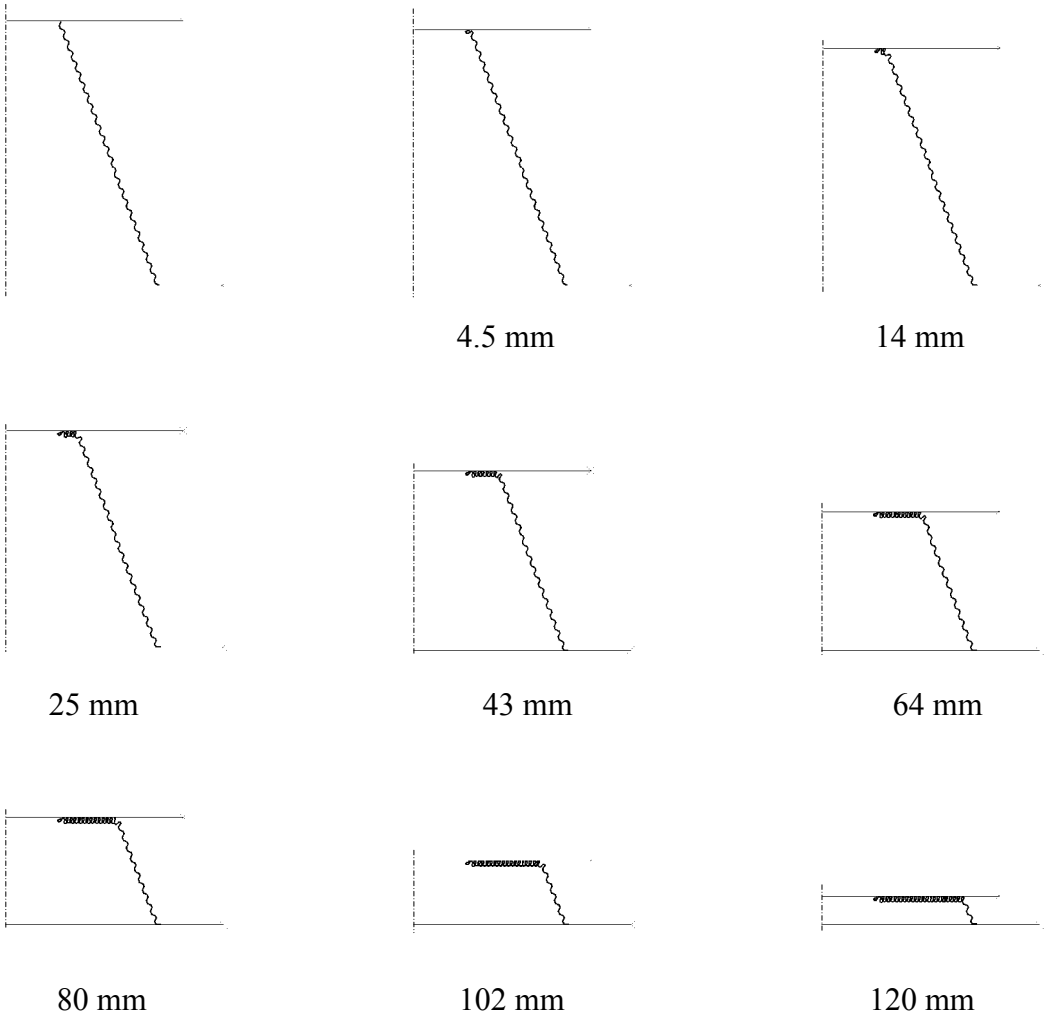

Fig.(11) Collapse mechanism of the 25 corrugations frustum model

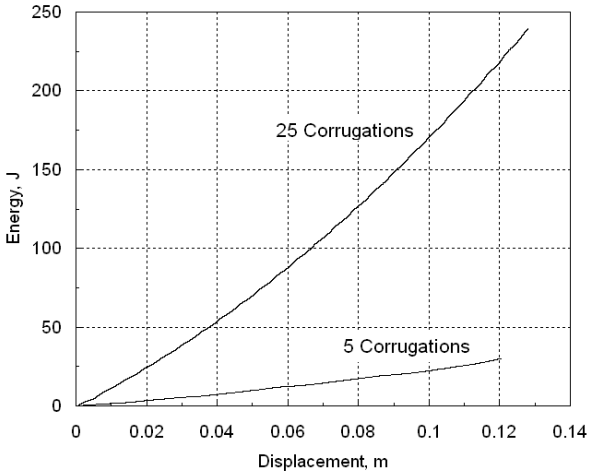

Fig.(12) Effect of the number of corrugations on the energy absorption capacity

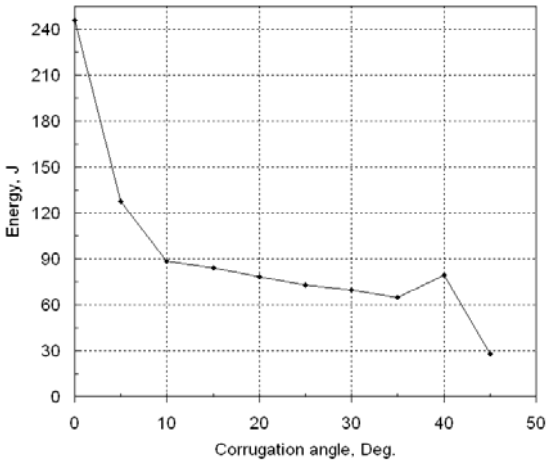

Fig.(13) Effect of the corrugation angle on the energy absorption capacity

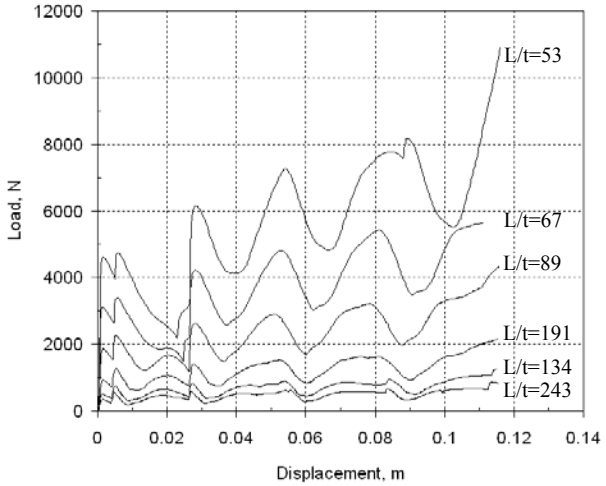

Fig.(14) Effect of the axial length-to-thickness ratio L/t on the load-displacement characteristics

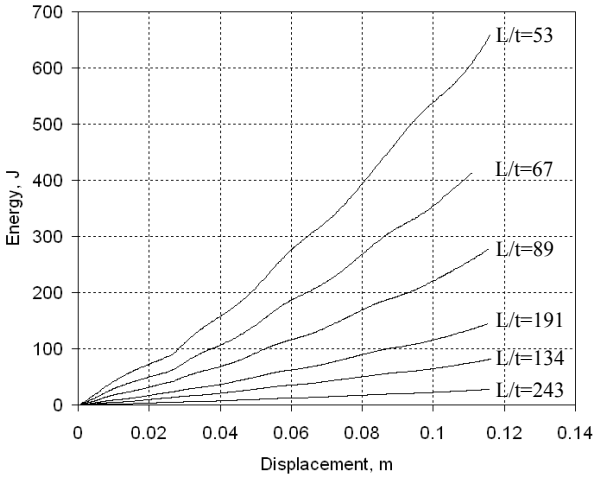

Fig.(15) Effect of the axial length-to-thickness ratio L/t on the energy absorption capacity

Table.(2) Comparison between presented numerical solution and experimental results in Ref.[8]

Parameters	Experimental	Numerical
Total compression (mm)	100	120
Peak load (kN)	5	4.7
Mean load (kN)	2.7	2.5
Absorbed energy (J)	300	250